Proceedings of the ASME 2023
ICE Forward Conference
ICEF2023
October 8-11, 2023, Pittsburgh, Pennsylvania

ICEF2023-110054

QUANTITATIVE VALIDATION OF A COMPUTATIONAL FLUID DYNAMICS METHODOLOGY FOR GASOLINE SPRAYS UNDER COLD START CONDITIONS

Dimitris Assanis[1,2,3,*,†], Joonsik Hwang[4,5,†], Gaurav Guleria[1,2], Dario Lopez-Pintor[6], Scott W. Wagnon[7], Russell Whitesides[7]

[1]Department of Mechanical Engineering, Stony Brook University, Stony Brook, NY
[2]Institute for Advanced Computational Science, Stony Brook, NY
[3]Advanced Energy Research and Technology Center, Stony Brook, NY
[4]Department of Mechanical Engineering, Mississippi State University, Mississippi State, MS
[5]Center for Advanced Vehicular Systems (CAVS), Starkville, MS
[6]Sandia National Laboratories, Livermore, CA
[7]Lawrence Livermore National Laboratory, Livermore, CA

ABSTRACT

Computational Fluid Dynamics (CFD) simulations have a great potential to guide the optimization of fuel stratification strategies for internal combustion engines, but well-validated spray models are required. In this study, we aim to understand the current capability of CFD simulations, under conditions representative of partially stratified advanced compression ignition engines, to predict gasoline sprays through quantitative comparisons based on liquid measurements. A series of backlit extinction imaging is carried out in a constant volume vessel under simulated engine-like cold start conditions. As a test fuel, regular E10 gasoline is injected using a commercial gasoline direct-injection (GDI) injector at two different injection pressures of 50 bar and 100 bar. High-speed imaging datasets were used to obtain quantitative measurements of the liquid penetration, and local liquid volume fraction from line-of-sight integration and computed tomographic reconstruction. Additionally, geometric information by x-ray computed tomography is provided to set initial and boundary conditions for the CFD simulations. Multidimensional large-eddy simulations (LES) of the gasoline fuel spray in a constant volume chamber are presented and compared to the experimentally obtained fundamental validation data. A well-validated surrogate fuel for regular E10 gasoline, called PACE-20, was used in the simulations. Detailed comparison between experiments and simulations shows faster spray development and evaporation of LES studies, leading to slightly longer liquid penetration lengths. Further, the numerical simulations were able to capture the strong plume collapsing of the tested injector under these conditions and to properly reproduce the experimental trends and the effects of injection pressure on the liquid spray.

NOMENCLATURE

Abbreviations

CFD	Computational Fluid Dynamics
CT	Computed Tomography
CO	Carbon Monoxide
DBIE	Diffused backlight illumination extinction
E10	Gasoline with 10% ethanol content by volume
GDI	Gasoline Direct Injection
HOV	Heat of Vaporization
IC	Internal Combustion
LED	Light Emitting Diode
LES	Large Eddy Simulations
LHV	Lower Heating Value
LLVF	Local liquid volume fraction
LTGC	Low-Temperature Gasoline Combustion
LVF	Liquid volume fraction
MON	Motor octane number
NVO	Negative Valve Overlap
NO_x	Nitrogen Oxides
PACE-20	Surrogate fuel for regular E10 gasoline
PLV	Projected liquid volume
PFS	Partial Fuel Stratification
PM	Particulate matter
RON	Research octane number
SOI	Start of injection
T10	10%vol evaporated temperature
T50	50%vol evaporated temperature
T90	90%vol evaporated temperature
TKE	Turbulent Kinetic Energy

[†]Joint first authors
[*]Corresponding author

UHC Unburned hydrocarbons

Greek letters

I transmitted attenuated light intensity

I_0 incident light intensity

τ Optical Thickness

1. INTRODUCTION

Low-temperature gasoline combustion (LTGC) engines can provide high efficiencies (similar to or even higher than those of modern diesel engines) with very low nitrogen oxides (NOx) and particulate matters (PM) emissions[1], but the absence of a simple and rapid mechanism to control the combustion timing remains as one of the main technical barriers for their commercial implementation [2]. In the last years, several techniques have been proposed and studied to overcome this challenge, such as trapping hot residual gases [3], injecting fuel during the negative valve overlap (NVO) [4], and spark assist [5]. However, these strategies are not fast enough, they are not suitable for low load operation or they penalize efficiency and/or emissions [5–8].

Partial fuel stratification (PFS) is one of the most promising techniques to control combustion under LTGC conditions [9]. This technique consists of injecting most of the fuel early during the intake stroke to create a background lean mixture, followed by a late direct fuel injection during the compression stroke to promote fuel stratification in the cylinder. The various local equivalence ratios within the stratified mixture will have different ignition delays [1, 10], leading to a sequential autoignition event in which, under typical LTGC engine conditions, the richer regions will ignite faster to control the combustion timing [11]. The amount of fuel stratification is adjusted by changing the injection settings of a gasoline-type direct injection system (GDI), such as the start of injection, providing control over the combustion on a cycle-to-cycle basis. Therefore, the fuel distribution in the cylinder results from a combination of the spray development of the late injection and the background mixture generated by the early injection, which is not necessarily homogeneous. The engine performance is heavily affected by this fuel distribution generated via PFS [12, 13]. Overly lean regions in the cylinder may lead to incomplete combustion and, therefore, decrease the engine efficiency and increase the emissions of carbon monoxide (CO) and unburned hydrocarbons (UHC). On the other hand, overly rich regions may lead to thermal NOx formation and, therefore, can also increase the overall NOx emissions.

It is unclear how the spray behavior would affect the ability of PFS to control the combustion at the wide range of injection conditions reached over the typical operating map of an engine, which ranges from cold, low ambient pressure conditions such as those of the intake stroke to high-temperature, high-pressure conditions such as those of the late compression stroke, especially at high engine loads. It is even more uncertain how the spray development would affect the performance of PFS under conditions in which spray collapse may occur. Spray collapse is particularly important for the early injection of fuel that typically occurs during the intake stroke, where the in-cylinder pressure may be low enough to lead to flash-boiling conditions. Thus, the early fuel injection may lead to unexpectedly heterogeneous background fuel distributions within the charge mixture, affecting the performance of PFS. Moreover, the effect of spray collapse on the spray development of the early fuel injection may lead to high spray-wall interactions that result in increasing soot emissions [14]. Unfortunately, little is known about spray collapse and spray development under LTGC-PFS conditions.

Computational Fluid Dynamics (CFD) simulations have shown a lot of potential to guide the optimization of PFS [15–18], but well-validated spray models are required to obtain reliable results. The validation of CFD spray simulations are typically performed using fundamental spray data obtained in constant volume [19] or constant-flow reaction chambers [20, 21]. Despite the fact that various databases for gasoline sprays using a gasoline direct injection (GDI) injector can be found in the literature, such as the Spray-G effort of the Engine Combustion Network [22, 23], results with regular E10 gasoline under conditions representative of PFS in an LTGC engine are not easily available. The objective of this study is to understand the current capability of CFD simulations, under PFS representative conditions, to predict gasoline sprays through quantitative comparisons based on well-characterized experimental measurements performed in a constant-volume chamber.

The structure of the paper is the following: first, the materials and methods are presented, including descriptions of the experimental facility, the optical diagnostics, and the CFD model and simulations. Then, the experimental results are discussed and compared against the CFD results for a quantitative evaluation of the numerical model. Finally, the conclusions of this investigation are drawn.

2. MATERIALS AND METHODS

2.1 High-speed extinction imaging setup

The spray experiments were carried out in a 1.4L constant volume chamber which has five (5) optical ports. For high-speed extinction imaging, a pair of parallel windows were used to take line-of-sight measurements. A schematic diagram and test image are shown in Figure 1.

The liquid spray was identified by diffused backlight illumination extinction (DBIE) imaging. A high-speed green light-emitting diode (LED), Fresnel lens (150 mm, f=150 mm), engineered diffuser, and band-pass filter (center wavelength: 527 nm, bandwidth: 20 nm, full width-half max: 22 nm) were utilized. A high-speed digital video camera (Phantom, v611) equipped with a prime lens (Nikkon, 50 mm f/5) was used to capture images of spray development in the vessel. The green LED was operated with a 1 ms command signal duration to freeze the spray in the visualized frame. The imaging was performed at a shutter speed of 21,000 frames per second (fps) with an image resolution of 512 by 512 pixels. The aperture of the lens and exposure time of the high-speed camera was set to 2.8 and 14.5 μs, respectively. The engineered diffuser supplied a homogeneous light field and suppressed beam steering by evaporation or temperature field in the vessel [24]. This imaging technique was designed to collect extinction only by the fuel in its liquid phase, yet not from the respective vapor. The injector was installed in the chamber with a rotating mount that enabled the precise angle alignment while providing a secure sealing of the chamber and fuel pressure. This allowed the viewing angle of the spray to be varied

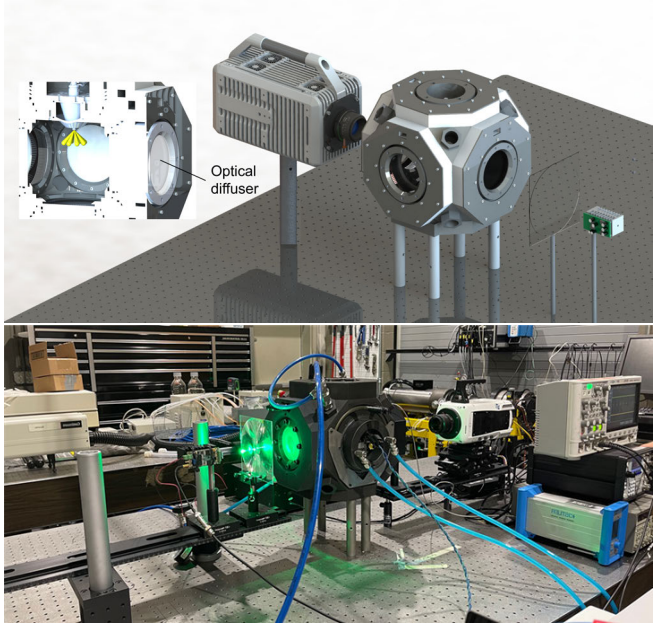

FIGURE 1: A SCHEMATIC DIAGRAM WITH OPTICAL COMPONENTS (TOP), AND AN IMAGE OF THE EXPERIMENTAL SETUP (BOTTOM).

with a fixed camera to obtain the projected liquid volume (PLV) images at different viewing angles needed for 3D computed tomography (CT) reconstruction. DBIE imaging was taken at 16 different viewing angles (injector rotating angle) from 0° to 180°, with 11.25-degree intervals while 10 injections were recorded for each injector position. The injector was rotated clockwise when looking at the nozzle tip. The 200 frames per injection covered a time span of about 3.0 ms including data during and after injection. Before each set, background (dark) frames were recorded with no lighting, and the initial intensity was measured for 20 frames prior to injection to evaluate reference illumination intensity pixel by pixel. This process should be completed within the count range of the camera (no zero or saturated pixels), making it possible to accurately measure the extinction signal.

2.2 Image processing method

Extinction imaging is known to be advantageous for spray characterization because it can provide more quantitative information for liquid fuel concentration than conventional Mie-scattering imaging associated with lighting and scattering uncertainties [25]. Using the measured optical thickness, droplet size, and extinction coefficient, the PLV along a line of sight can be derived for direct comparison with CFD results. The optical thickness in a spray region can be calculated based on Beer-Lambert law as follows in Eqn. 1:

$$\tau = -\ln\left(\frac{I}{I_0}\right) \tag{1}$$

where I is transmitted attenuated light intensity due to interaction with the liquid spray, and I_0 is incident light intensity without any extinction. This level of transmission intensity is reasonable for detection of the spray outline above the noise floor of the camera, but the vapor-phase beam steering needs to be considered and accounted for using engineered diffusers [24]. The measured optical thickness, τ, is correlated to the PLV, which is the integral of liquid volume fraction (LVF) along the cross-stream direction y, as follows:

$$\mathbf{PLV} = \tau \cdot \frac{\pi \cdot d^{3/6}}{C_{ext}} = \int_{-y_\infty}^{y_\infty} \mathbf{LVF} \cdot dy \tag{2}$$

Mie-scattering and extinction theories were applied in Eqn. 2, along with assumptions that droplet diameter d and extinction coefficient C_{ext} do not vary along the line of sight. The PLV indicates how much liquid volume is in a certain projected area, so it has a unit of mm^3(liquid)/mm^2. To derive PLV quantitatively, the important parameters such as d and C_{ext} should be quantified. In particular, C_{ext} is a function of droplet size, a wavelength of light, and a collection angle of the receiving optics. In this study, droplet diameter was assumed to be 7 µm with fair uniformity across the plume during injection as applied in the previous studies on PLV quantification of GDI spray [21, 26]. Then, the C_{ext} was calculated as 72.70-6 mm^2 using MiePlot [27]. Figure 2 illustrates the image-processing techniques applied to quantify the spray's projected liquid volume. Starting from the brightness of an image under evaluation, ensemble-averaged was normalized using a background image absent of spray. Subsequently, averaged and corrected intensity values were then translated into PLV values using Eqn. (2).

As discussed above, PLV data with 16 different viewing angles were transformed into 3D spray by a computed tomography (CT) algorithm. A sinogram was built by stacking the extracted z-plane PLV profile from each viewing angle as shown in Figure 3.

Since the PLV data were available at 16 viewing angles from 0° to 180°, the 'full view' CT reconstruction could be conducted in contrast to the author's previous studies in which 'limited view' tomography was performed [21, 26]. The reconstruction was carried out by using a built-in 'iradon' function in MATLAB which uses the filtered back-projection algorithm to perform the inverse Radon transform. The reconstruction routine was applied at 15 mm and 30 mm from the nozzle while the Hamming filter of 0.6 was used.

2.3 Experimental conditions

The spray experiments were carried out under simulated cold start condition keeping ambient and fuel at 25°C using a GDI injector that has 8 axis-symmetric nozzles. It is noted that this is non-reacting condition with only nitrogen gas in ambient. The injection command with a duration of 1 ms with injection pressure of 50 bar, and 100 bar. 16 different injector viewing angles with 11.25° interval were applied and the spray was repeated 10 times per case for extinction imaging. The resulting spray plume angle was determined from the x-ray imaging. Additionally, the injector rate profile was determined using a custom in-house machine learning algorithm [28] and shown in Fig. 4.

2.4 Computational setup

Three-dimensional Large-eddy Simulations (LES) using CONVERGE (v3.0) [29] were performed to investigate prefer-

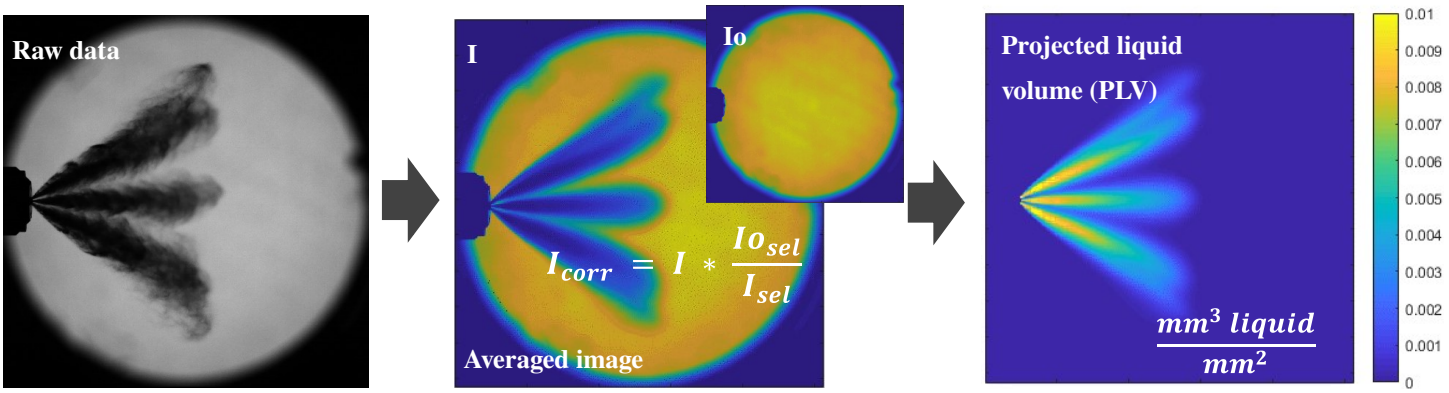

FIGURE 2: PROCEDURES TO ACQUIRE PROJECTED LIQUID VOLUME (PLV) MAP FROM RAW EXTINCTION IMAGE.

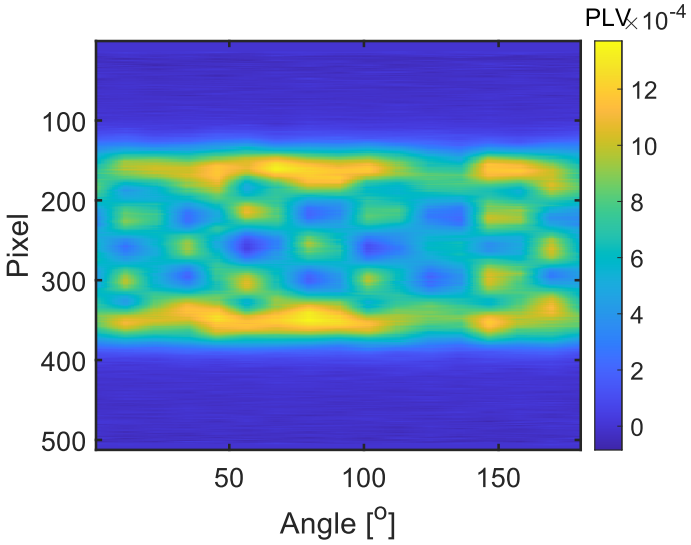

FIGURE 3: SINOGRAM FOR LIQUID VOLUME FRACTION RECONSTRUCTION.

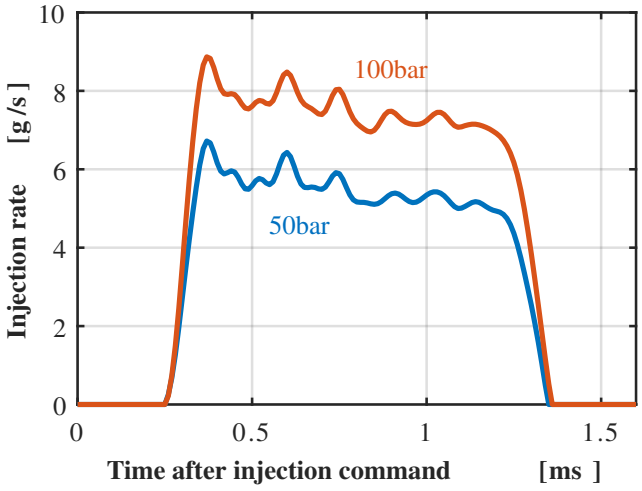

FIGURE 4: INJECTOR RATE PROFILE AT 50 AND 100 BAR INJECTION PRESSURE.

TABLE 1: PACE-20 COMPOSITION IN LIQUID VOLUME FRACTIONS.

Species	LVF [%]
N-pentane	0.1395
N-heptane	0.1153
Iso-octane	0.2505
Cyclo-pentane	0.1050
Toluene	0.0919
1,2,4-Trimethylbenzene	0.1187
Tetralin	0.0295
1-Hexene	0.0541
Ethanol	0.0955

ential evaporation with PACE-20, the gasoline surrogate fuel. Turbulent eddies of different length scales are formed during spray phenomena that must be considered to accurately resolve the spray injection and spray breakup events. LES was preferred over RANS modeling as RANS models do not resolve the eddy energy spectrum. For the current study, a LES model, the Dynamic Structure model with Favre filtering, is used to model turbulence with a sufficiently small grid size to resolve the eddy energy spectrum.

The surrogate fuel PACE-20 was developed as a joint effort within the United States (U.S.) Department of Energy (DOE) Partnership to Advance Combustion Engines (PACE) consortium, and it has shown to match the autoignition reactivity, octane rating, distillation characteristics, laminar burning velocity, spray behavior, soot propensity and engine behavior of the real fuel [30], [31].The PACE-20 is a 9-component surrogate designed to replicate both the physical and chemical properties of a research-grade regular E10 gasoline. The composition of PACE-20 is shown in Table 1. The main properties of both PACE-20 and the research-grade regular E10 gasoline are shown in Table 2. Finally, the distillation curve measured according to ASTM D86 Distillation of Petroleum Products and Liquid Fuels at Atmospheric Pressure test of both PACE-20 and the full-boiling range gasoline are shown in Figure 5.

The phenomena being studied in the current study is spray. During the spray injection and spray breakup events, turbulent

TABLE 2: MAIN PROPERTIES OF PACE-20 AND A RESEARCH-GRADE REGULAR E10 GASOLINE.

Property	PACE-20	Regular E10 gasoline
RON	92.1	92.3
MON	84.5	84.6
H/C ratio	1.964	1.969
Density at 15°C [g/mL]	0.742	0.750
LHV [MJ/kg]	41.71	41.77
PMI	1.51	1.68
HOV [kJ/kg]	407.5	419.9

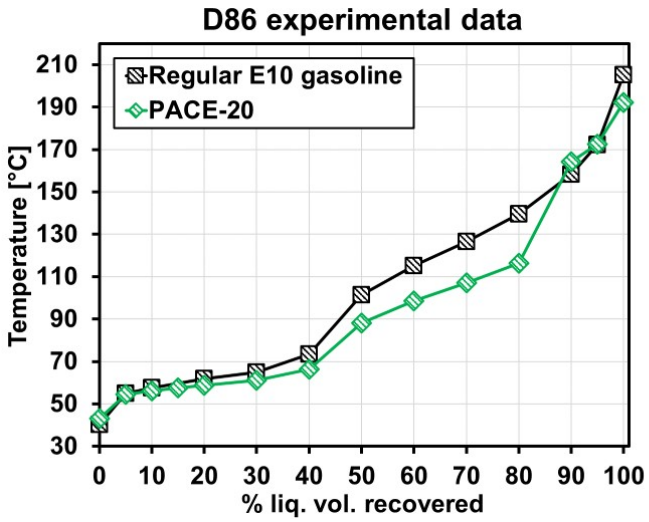

FIGURE 5: ASTM D86 DISTILLATION CURVE OF PACE-20 AND A RESEARCH-GRADE REGULAR E10 GASOLINE.

eddies of different length scales are formed. LES was preferred over RANS modeling as RANS models do not resolve the eddy energy spectrum. For the current study, a LES model with a sufficiently small grid size was used to resolve the eddy energy spectrum. The turbulence model used was the Dynamic Structure model with Favre filtering. Further details on gird size selection are described later.

Simulations were performed under non-reacting cold start conditions with a N_2 ambient. The simulations had matching conditions to those of the experiments. The injector inputs, for example number of nozzle holes, plume direction angle, nozzle diameter was provided by x-ray computed tomography as shown in Figure 6. An injection rate profile provided by a machine-learning based model was used for the simulation [28]. The simulation time was set up to 2 ms after the start of injection (SOI). The plume direction angle of 25° has been defined as an input based on the previous research [21]. The maximum grid resolution is 125 μm in the adaptive mesh refinement (AMR) and fixed embedding regions. AMR is activated based on velocity gradients. The fix embedding zone is a 10 mm length cone centered on the injector, with a first radius of 2 mm at the nozzle tips and a second radius of 5 mm downstream. The model constants for the spray sub-models were set up on the basis of ECN Spray G experiments [32]. More details on the numerical setup, including the choice of the models used to capture spray breakup and vaporization, can be found in Table 3. Specifically, the KH-RT break-up model is selected for use in this study for breakup on the basis of consistently good performance for accurately predicting the spray breakup of gasoline sprays as detailed by Som et al. [33] and Senecal et al. [34]. Figure 7 shows the final mesh size of the domain at 1.8 ms after the start of injection. The computational time required for the runs will be discussed in detail in the results and discussion section of the study.

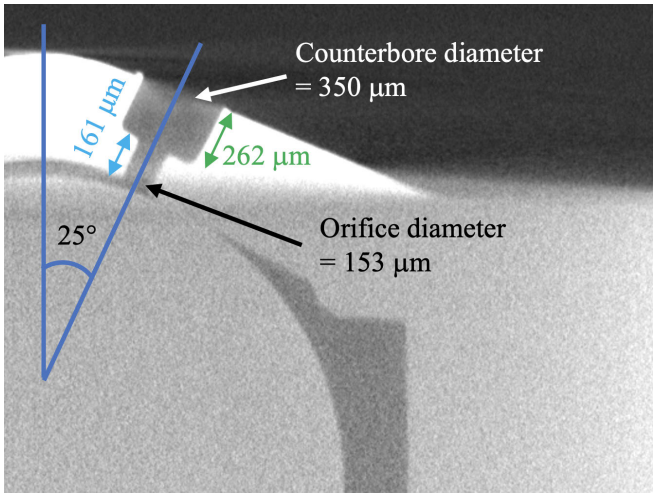

FIGURE 6: X-RAY IMAGE OF TEST INJECTOR.

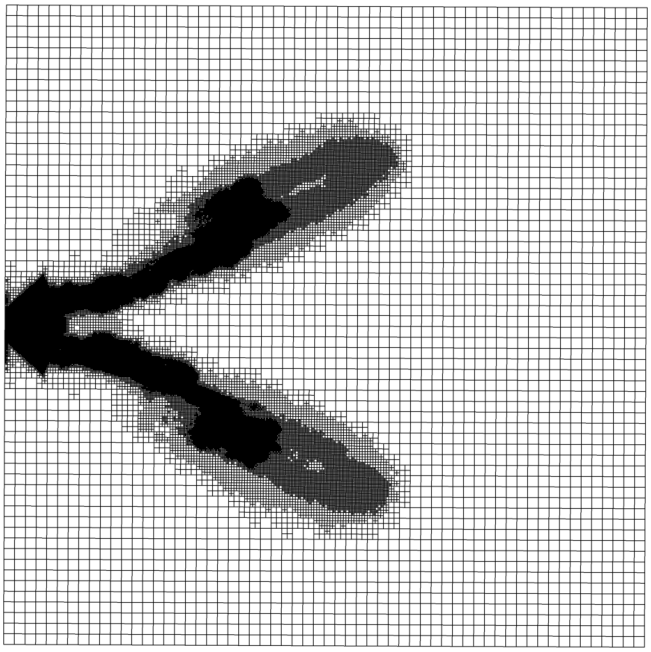

FIGURE 7: CUT PLANE OF THE COMPUTATIONAL DOMAIN SHOWING THE FINAL GRID USED FOR THE STUDY AT 1.8 MS ASOI.

TABLE 3: COMPUTATIONAL SETUP AND PHYSICAL MODEL SELECTION.

CFD CODE AND GRID INFORMATION	
CFD code	CONVERGE 3.0
Grid Type	AMR and fixed embedding
Base grid [mm]	2.0
Embedding level	4
AMR level	4 (based on velocity)
Max. resolution [mm]	0.125
MODELS	
Turbulence	LES dynamic structure
Spray model	Lagrangian parcel 145,000 - 210,000 parcels per nozzle)
Injection	BLOB (diameter initial parcels = nozzle diameter)
Breakup model	KH-RT (B0= 0.6 and B1= 5)
Vaporization	Frossling
Droplet collision	No time counter (NTC)
Droplet drag	Dynamic sphere
Droplet dispersion	O'Rourke

3. RESULTS AND DISCUSSION

3.1 Computational and Experimental Result Comparison

Projected liquid volume comparison between experiment and CFD simulation is shown in Figure 8. The experimental value was calculated by Eqn. (2). The PLV from CFD simulation was also calculated by identical method. It can be seen that this injector showed a strong plume collapsing even though the ambient and fuel temperature was low (cold condition).

Individual plumes were merged together and left intense PLV signal in the center of the spray. Especially under 100 bar condition when plume got thicker, results showed earlier plume collapsing and specific vortical structure in the leading edge. The CFD simulation indicated collapsing and similar overall spray morphology compared to the experimental data. In overall, the plume dynamics were also able to be captured.

For quantitative comparison, liquid length also calculated using the line-of-sight PLV measurement with PLV threshold of 0.2x10-3 mm3(liquid)/mm2 for both experiment and CFD simulation. The liquid length result is shown in Figure 9.

As it could be predicted by the previous PLV map shown in Figure 6, CFD simulations had similar spray development at early timings, but ultimately showed slightly longer penetration distance than the experiments, as shown in Figure **??**. The CFD simulation results showed ~4-5 mm longer liquid penetration than the experimental results for both 50 bar and 100 bar injection pressures. It is possible that the evaporation model is underpredicting the liquid to gas phase transition of the fuel and thus a larger portion of the spray remains in liquid phase for a longer period of time. This would contribute to the longer spray penetration results predicted by the CFD simulations versus what is observed in the physical experiments. Further parameter tuning of the spray evaporation model could help resolve this discrepancy that is noted between CFD results and the validation experiments.

For more detailed comparison, local liquid volume fraction (LLVL) was compared between experiment and CFD simulation. Figure 8 presents liquid volume fraction at 15 mm and 30 mm with 50 bar and 100 bar conditions. It is noted that the experimental data indicates local liquid volume fraction enabled by 3D CT. At 1ms after start of injection, plumes were merged together by strong plume-to-plume interactions. As confirmed in the line-of-sight measurement, stronger plume merging was detected with higher injection pressure case showing narrower profile of LVF at cut plane. The CFD simulation had more plume collapsing under 100 bar condition showing higher level of LVF at the center of the spray. The plumes in CFD at the 15 mm plane showed relatively larger individual plumes than the experiment, however, at 30 mm plane, it showed good agreement not only for plume size, but also location. As this simulation is Lagrangian parcel simulation, the local LVF is not continuous by its nature, but CFD simulation showed similar level of local LVF compared to the experiment.

A few other discrepancies to note that may explain computational and experimental result mismatches are as follows. In the experiments, gasoline is used for injection. The PACE-20 surrogate has physical properties very similar to the real gasoline E10 fuel, however, it can be seen from Figure 5 there is still some difference between the distillation curve of regular E10 gasoline and PACE-20 surrogate. It is reasonable to believe that this can explain some of the discrepancies observed in the modeling results. Another cause of computational uncertainty can be the decision to use the Spray G experimental data for the spray sub models as the injector used for the current study is not exactly the same as Spray G injector. However, considering the long computation time for these runs that is described in further detail in the next section, the authors agreed to use the Spray G spray sub models constants instead of running sensitivity analysis of different spray sub model constants. This approach was decided and deemed reasonable since the Spray G Delphi 8 hole GDI injector is similar to the injector used in the current study.

3.2 Computational Model Parameters Trade-offs

Through the course of this work, the authors found the computational results to be highly dependent on the computational model parameters presented. Grid independence studies could not be classically performed as LES require a specific fine grid size to ensure that enough of the turbulent kinetic energy is being resolved. In their work, Rutland [35] have shown that for engineering LES studies resolving 60-80% of the flow kinetic energy is sufficient for internal combustion (IC) engines.

Some of the computational limitations encountered are detailed below. Once the domain reached the 20 million cell limit, the the sub-grid scale (SGS) of the velocity started to increase, as seen in 11 as the 100 bar case required higher parcel count. Best practice recommendations are to keep the SGS velocities under a range of 0.5-1.0 m/sec, which was accomplished for both the modeling runs.

The results presented are highly dependent on computational model parameter.

Additionally, there is a trade off between number of parcels, mesh size, and computational resources required. As the mesh

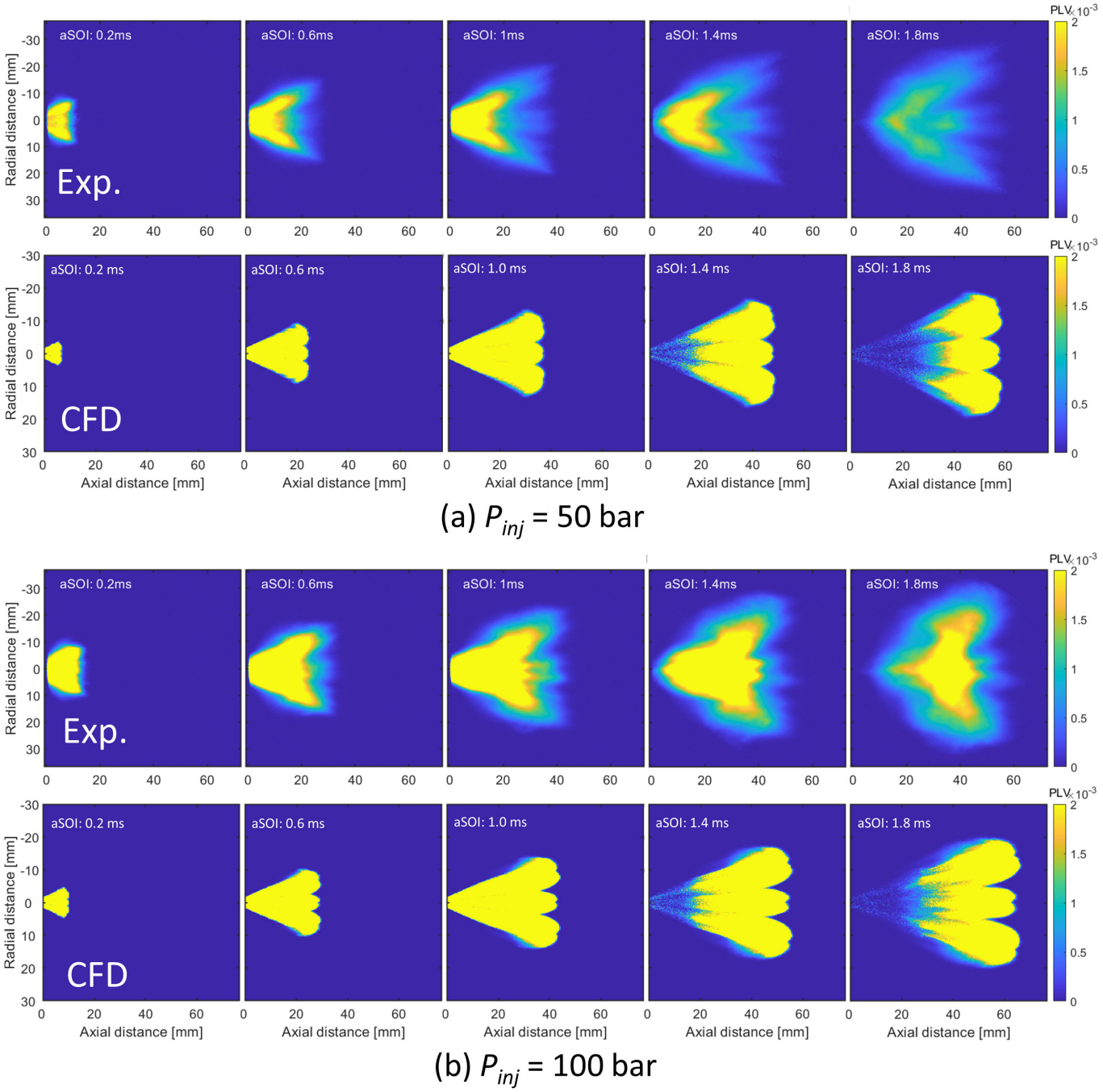

FIGURE 8: COMPARISON OF PROJECTED LIQUID VOLUME AT (A) 50 BAR FUEL INJECTION PRESSURE, AND (B) 100 BAR FUEL INJECTION PRESSURE TOP: EXPERIMENT, BOTTOM: CFD SIMULATION.

size needs to be fine enough to resolve a substantial portion of the turbulent kinetic energy (TKE) for the LES computations, the number of parcels needs to be increased exponentially to make sure the spray penetration in not over predicted due to more mass being injected in lesser number of parcels and to maintain adequate spray resolution. Runs up to 580,000-840,000 parcels per nozzle with a base grid size of 0.0625mm were trialed and could be computed, albeit at unreasonably long turn around times of more than 3 weeks per injection event. Attempting to perform a grid independence study at half the base cell mesh size of 0.03125 mm would require a quadrupling of the parcel count to the tune of 2,320,000-3,360,000 parcels per nozzle, which would entirely be computationally prohibitive with reasonable academic high performance computing (HPC) resources.

Ultimately values of 120,000-250,000 parcels per nozzle were feasible to be solved using 250-300 cores and around 10 days of computational run time. 120,0000 parcels per nozzle provided adequate, but not sufficient matching to the experimental results, but 145,000-210,000 parcels per nozzle, a base mesh size of 2 mm with level 4 fixed embedding and AMR running on

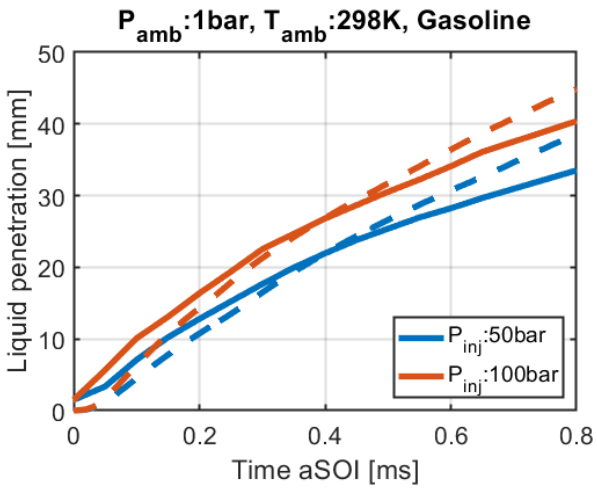

FIGURE 9: LIQUID PENETRATION COMPARISON BETWEEN EXPERIMENT (SOLID LINE) AND CFD (DASHED LINES) SIMULATION AT 50 AND 100 BAR INJECTION PRESSURE CONDITIONS.

250 cores allowed for the results in Figures 6-10 to be determined.

It is clear that a trade-off between computational accuracy and the amount of computational resources required exists. Ultimately, the above mentioned settings are a good compromise to the technical conundrum created between reducing computational expense at the cost of decreasing model accuracy and still maintaining enough fidelity to capture the major physics involved in computationally representing the physical spray phenomena.

4. SUMMARY AND CONCLUSIONS

In this study, a detailed quantitative comparison method between experimental studies and CFD simulation is established. In the physical experiments, detailed information of projected liquid volume and local liquid volume fraction were derived by line-of-sight integration and computed tomographic reconstruction, respectively. Additionally, high-resolution x-ray CT for the injector geometry was carried out to deliver precise inputs required for the computational studies. The high-speed extinction imaging provided good spatial-temporal spray information for quantitative CFD validation. We tested this method in a GDI spray and validated the comparison approach. Detailed comparison showed similar spray development and evaporation than that of what was predicted by the LES modeling results. The computational results show slightly longer liquid penetration length and width at later injection timings, however, the LES simulation results were able to capture the strong plume collapsing of the experimentally tested injector. The study showed that using 580,000-840,000 parcels per nozzle with a grid size of 0.0625 mm take around 3 weeks of run-time per simulation. For the grid size of 0.125 mm with 145,000-210,000 parcels per nozzle allowed decent agreement with the experimental data with around 10 days of computational time. This study ultimately outlines a methodology that allows for a level of understanding to be gained by performing quiescent constant volume experiments to help improve the confidence interval of a selected spray model and the use of default parameters to characterize and validate 3D CFD spray modeling for use in engine applications.

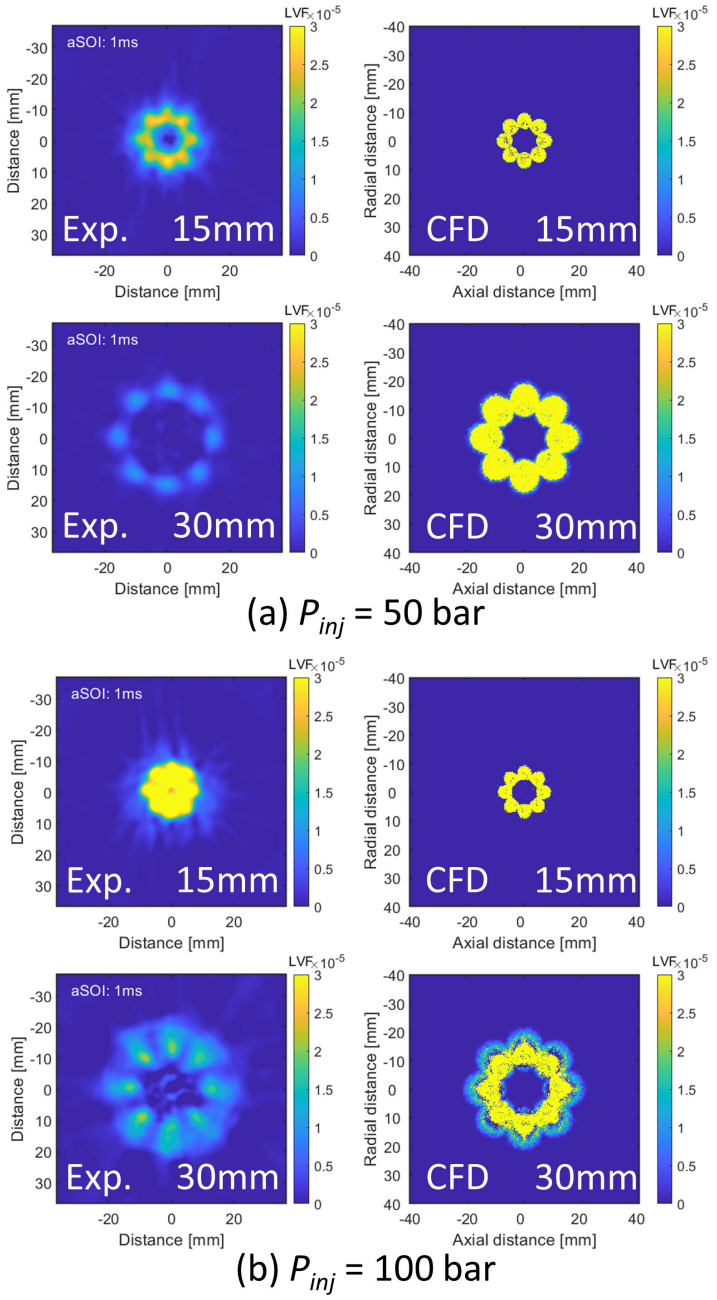

FIGURE 10: LOCAL LIQUID VOLUME FRACTION AT 15 MM AND 30 MM WITH AN INJECTION PRESSURE OF (A) 50 BAR, AND (B) 100 BAR AT 1 MS ASOI. EXPERIMENTAL RESULT PRESENTED IN THE LEFT COLUMN, AND THE CFD IS SHOWN IN THE RIGHT COLUMN.

ACKNOWLEDGMENTS

All of the experimental work and related data analysis were performed at the Center for Advanced Vehicular System (CAVS) of Mississippi State University. The authors would like to thank Stony Brook Research Computing and Cyberinfrastructure, and the Institute for Advanced Computational Science at Stony Brook University for access to the high-performance SeaWulf computing system, which was made possible by a $1.4M National Science Foundation grant (#1531492). Convergent Science provided CONVERGE licenses and technical support for this work. Work

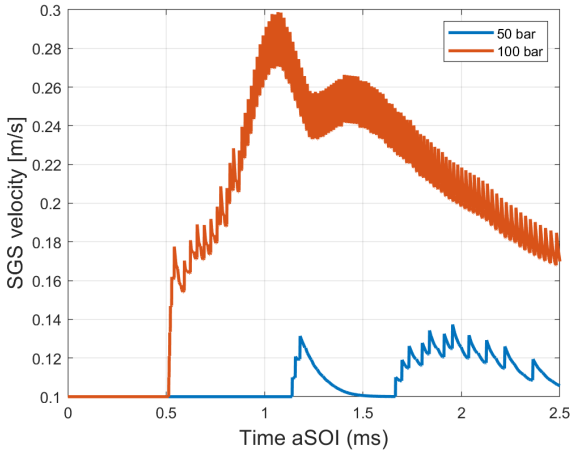

FIGURE 11: SUB-GRID SCALE VELOCITIES STAYED BELOW THE RECOMMENDED 0.5 M/SEC VELOCITY.

at LLNL was performed under the auspices of the U.S. Department of Energy (DOE) under Contract DE-AC52-07NA2734 as part of the Partnership to Advance Combustion Engines (PACE) sponsored by the U.S. DOE Vehicle Technologies Office (VTO).

REFERENCES

[1] Dec, JE and Lopez-Pintor, D. "Demonstrating the Potential of LTGC-AMFI to Deliver the Promise of Low-Temperature Combustion." *Thermo and Fluid Dynamic Processes in Direct Injection Engines THIESEL, Valencia, Spain* (2020).

[2] Dec, John E. "Advanced compression-ignition engines—understanding the in-cylinder processes." *Proceedings of the combustion institute* Vol. 32 No. 2 (2009): pp. 2727–2742.

[3] Koopmans, Lucien and Denbratt, Ingemar. "A four stroke camless engine, operated in homogeneous charge compression ignition mode with commercial gasoline." *SAE Transactions* (2001): pp. 2324–2337.

[4] Fitzgerald, Russell P and Steeper, Richard. "Thermal and chemical effects of NVO fuel injection on HCCI combustion." *SAE international journal of engines* Vol. 3 No. 1 (2010): pp. 46–64.

[5] Ji, Chunsheng, Dernotte, Jeremie, Gentz, Gerald and Dec, John. "Spark Assist for CA50 Control and Improved Robustness in a Premixed LTGC Engine – Effects of Equivalence Ratio and Intake Boost." *WCX World Congress Experience*. 2018. SAE International. DOI https://doi.org/10.4271/2018-01-1252. URL https://doi.org/10.4271/2018-01-1252.

[6] Dec, John E. and Sjöberg, Magnus. "A Parametric Study of HCCI Combustion - the Sources of Emissions at Low Loads and the Effects of GDI Fuel Injection." *SAE 2003 World Congress & Exhibition*. 2003. SAE International. DOI https://doi.org/10.4271/2003-01-0752. URL https://doi.org/10.4271/2003-01-0752.

[7] Borgqvist, Patrick, Tunestal, Per and Johansson, Bengt. "Comparison of Negative Valve Overlap (NVO) and Rebreathing Valve Strategies on a Gasoline PPC Engine at Low Load and Idle Operating Conditions." *SAE International Journal of Engines* Vol. 6 No. 1 (2013): pp. 366–378. DOI https://doi.org/10.4271/2013-01-0902. URL https://doi.org/10.4271/2013-01-0902.

[8] Yun, Hanho, Wermuth, Nicole and Najt, Paul. "Development of Robust Gasoline HCCI Idle Operation Using Multiple Injection and Multiple Ignition (MIMI) Strategy." *SAE World Congress & Exhibition*. 2009. SAE International. DOI https://doi.org/10.4271/2009-01-0499. URL https://doi.org/10.4271/2009-01-0499.

[9] Sjöberg, Magnus and Dec, John E. "Smoothing HCCI Heat-Release Rates Using Partial Fuel Stratification with Two-Stage Ignition Fuels." *SAE 2006 World Congress & Exhibition*. 2006. SAE International. DOI https://doi.org/10.4271/2006-01-0629. URL https://doi.org/10.4271/2006-01-0629.

[10] Lopez Pintor, Dario, Dec, John and Gentz, Gerald. "ϕ-Sensitivity for LTGC Engines: Understanding the Fundamentals and Tailoring Fuel Blends to Maximize This Property." *WCX SAE World Congress Experience*. 2019. SAE International. DOI https://doi.org/10.4271/2019-01-0961. URL https://doi.org/10.4271/2019-01-0961.

[11] Lopez Pintor, Dario, Dec, John and Gentz, Gerald. "Experimental Evaluation of a Custom Gasoline-Like Blend Designed to Simultaneously Improve ϕ-Sensitivity, RON and Octane Sensitivity." *SAE International Journal of Advances and Current Practices in Mobility* Vol. 2 No. 4 (2020): pp. 2196–2216. DOI https://doi.org/10.4271/2020-01-1136. URL https://doi.org/10.4271/2020-01-1136.

[12] Dernotte, Jeremie, Gentz, Gerald, Ji, Chunsheng, Lopez Pintor, Dario and Dec, John. "Combustion-Timing Control of Low-Temperature Gasoline Combustion (LTGC) Engines by Using Double Direct-Injections to Control Kinetic Rates." *WCX SAE World Congress Experience*. 2019. SAE International. DOI https://doi.org/10.4271/2019-01-1156. URL https://doi.org/10.4271/2019-01-1156.

[13] Lopez Pintor, Dario, Gentz, Gerald and Dec, John. "Mixture Stratification for CA50 Control of LTGC Engines with Reactivity-Enhanced and Non-Additized Gasoline." *SAE WCX Digital Summit*. 2021. SAE International. DOI https://doi.org/10.4271/2021-01-0513. URL https://doi.org/10.4271/2021-01-0513.

[14] Kim, Namho, Vuilleumier, David and Sjoberg, Magnus. "Effects of Injection Timing and Duration on Fuel-Spray Collapse and Wall-Wetting in a Stratified Charge SI Engine." *SAE WCX Digital Summit*. 2021. SAE International. DOI https://doi.org/10.4271/2021-01-0544. URL https://doi.org/10.4271/2021-01-0544.

[15] Guleria, Gaurav, Lopez-Pintor, Dario, Dec, John E and Assanis, Dimitris. "A comparative study of gasoline skeletal mechanisms under partial fuel stratification conditions using large eddy simulations." *International Journal of Engine Research* Vol. 23 No. 10 (2022): pp. 1658–1677. DOI 10.1177/14680874211031370. URL https://doi.org/10.1177/14680874211031370.

[16] Guleria, Gaurav, Lopez-Pintor, Dario, Dec, John E and Assanis, Dimitris. "Development and evaluation of a skele-

tal mechanism for EHN additized gasoline mixtures in large Eddy simulations of HCCI combustion." *International Journal of Engine Research* Vol. 0 No. 0 (0): p. 14680874231178099. DOI 10.1177/14680874231178099. URL https://doi.org/10.1177/14680874231178099.

[17] Priyadarshini, Priya, Sofianopoulos, Aimilios, Mamalis, Sotirios, Lawler, Benjamin, Lopez-Pintor, Dario and Dec, John E. "Understanding partial fuel stratification for low temperature gasoline combustion using large eddy simulations." *International Journal of Engine Research* Vol. 22 No. 6 (2021): pp. 1872–1887. DOI 10.1177/1468087420921042. URL https://doi.org/10.1177/1468087420921042.

[18] Desantes, José, A-Oliver, José, Novella, Ricardo, Pastor, Jose, Shang, Weiwei, Bensalem, Chafik and Lopez-Pintor, Dario. "Application of a Coupled Eulerian Spray Approach and a Flamelet-based Combustion Model to Single Hole Primary Reference Fuel Sprays." 2020.

[19] Singh, Akhilendra Pratap, Shukla, Pravesh Chandra, Hwang, Joonsik and Agarwal, Avinash Kumar. *Introduction to Combustion Simulations and Optical Diagnostic Techniques for Internal Combustion Engines*. Springer Singapore, Singapore (2020): pp. 3–6. DOI 10.1007/978-981-15-0335-1_1. URL https://doi.org/10.1007/978-981-15-0335-1_1.

[20] Oh, Heechang, Hwang, Joonsik, White, Logan, Pickett, Lyle M. and Han, Donghee. "Spray collapse characteristics of practical GDI spray for lateral-mounted GDI engines." *International Journal of Heat and Mass Transfer* Vol. 190 (2022): p. 122743. DOI https://doi.org/10.1016/j.ijheatmasstransfer.2022.122743. URL https://www.sciencedirect.com/science/article/pii/S0017931022002253.

[21] Hwang, Joonsik, Weiss, Lukas, Karathanassis, Ioannis K., Koukouvinis, Phoevos, Pickett, Lyle M. and Skeen, Scott A. "Spatio-temporal identification of plume dynamics by 3D computed tomography using engine combustion network spray G injector and various fuels." *Fuel* Vol. 280 (2020): p. 118359. DOI https://doi.org/10.1016/j.fuel.2020.118359. URL https://www.sciencedirect.com/science/article/pii/S0016236120313557.

[22] Engine Combustion Network. "Engine Combustion Network." https://ecn.sandia.gov/. (Accessed on 04/15/2023).

[23] Gutierrez, Luis, Mansfield, Andrew B., Fatouraie, Mohammad, Assanis, Dimitris, Singh, Ripudaman, Lacey, Joshua, Brear, Michael and Wooldridge, Margaret. "Effects of Engine Speed on Spray Behaviors of the Engine Combustion Network "Spray G" Gasoline Injector." *WCX World Congress Experience*. 2018. SAE International. DOI https://doi.org/10.4271/2018-01-0305. URL https://doi.org/10.4271/2018-01-0305.

[24] Westlye, Fredrik R., Penney, Keith, Ivarsson, Anders, Pickett, Lyle M., Manin, Julien and Skeen, Scott A. "Diffuse back-illumination setup for high temporally resolved extinction imaging." *Appl. Opt.* Vol. 56 No. 17 (2017): pp. 5028–5038. DOI 10.1364/AO.56.005028. URL https://opg.optica.org/ao/abstract.cfm?URI=ao-56-17-5028.

[25] Pickett, Lyle M., Genzale, Caroline L. and Manin, Julien. "UNCERTAINTY QUANTIFICATION FOR LIQUID PENETRATION OF EVAPORATING SPRAYS AT DIESEL-LIKE CONDITIONS." *Atomization and Sprays* Vol. 25 No. 5 (2015): pp. 425–452.

[26] Weiss, Lukas, Wensing, Michael, Hwang, Joonsik, Pickett, Lyle and Skeen, Scott. "Development of limited-view tomography for measurement of Spray G plume direction and liquid volume fraction Graphic abstract." *Experiments in Fluids* Vol. 61 (2020): p. 51. DOI 10.1007/s00348-020-2885-0.

[27] Philip Laven. "MiePlot." http://www.philiplaven.com/mieplot.htm. (Accessed on 04/15/2023).

[28] Oh, Heechang, Hwang, Joonsik, Pickett, Lyle M. and Han, Donghee. "Machine-learning based prediction of injection rate and solenoid voltage characteristics in GDI injectors." *Fuel* Vol. 311 (2022): p. 122569. DOI https://doi.org/10.1016/j.fuel.2021.122569. URL https://www.sciencedirect.com/science/article/pii/S0016236121024376.

[29] Richards, K.J., Senecal, P.K. and Pomraning, E. "CONVERGE 3.0." 2023, Convergent Science, Madison, WI.

[30] Wagnon, S. W. "Development of an Optimized Gasoline Surrogate Formulation for PACE Experiments and Simulations." Technical report no. U.S. Department of Energy Vehicles Technology Office. 2021. URL https://www.energy.gov/sites/default/files/2021-07/VTO_2020_APR_ADV_FUEL_COMPILED_REPORT_JUL_7_2021_compliant_.pdf.

[31] Cheng, Song, Goldsborough, S. Scott, Wagnon, Scott W., Whitesides, Russell, McNenly, Matthew, Pitz, William J., Lopez-Pintor, Dario and Dec, John E. "Replicating HCCI-like autoignition behavior: What gasoline surrogate fidelity is needed?" *Applications in Energy and Combustion Science* Vol. 12 (2022): p. 100091. DOI https://doi.org/10.1016/j.jaecs.2022.100091. URL https://www.sciencedirect.com/science/article/pii/S2666352X22000346.

[32] Manin, Julien, Jung, Yongjin, Skeen, Scott A, Pickett, Lyle M, Parrish, Scott E and Markle, Lee. "Experimental characterization of DI gasoline injection processes." Technical report no. SAE Technical Paper. 2015.

[33] Som, Sibendu, Wang, Zihan, Pei, Yuanjiang, Senecal, Peter Kelly and Pomraning, Eric. "LES of Vaporizing Gasoline Sprays Considering Multi-Injection Averaging and Grid-Convergent Mesh Resolution." *Internal Combustion Engine Division Fall Technical Conference*, Vol. 57281: p. V002T06A002. 2015. American Society of Mechanical Engineers.

[34] Senecal, PK, Pomraning, Eric, Richards, KJ and Som, Sibendu. "An investigation of grid convergence for spray simulations using an LES turbulence model." Technical report no. SAE Technical Paper. 2013.

[35] Rutland, CJ. "Large-eddy simulations for internal combustion engines–a review." *International Journal of Engine Research* Vol. 12 No. 5 (2011): pp. 421–451.